Two-magnon bound states and their oscillating deconfinement crossover in two and three dimensions

Zhao-Yang Dong [1] and Jian-Xin Li[2,3,*]

[1]*Department of Applied Physics, Nanjing University of Science and Technology, Nanjing 210094, China*
[2]*National Laboratory of Solid State Microstructures and Department of Physics, Nanjing University, Nanjing 210093, China*
[3]*Collaborative Innovation Center of Advanced Microstructures, Nanjing University, Nanjing 210093, China*

Confinement is a ubiquitous phenomenon in which constituent particles are bound together into a new quasiparticle. In condensed matter physics, magnon bound states can be regarded as a confinement of magnons, and an oscillating deconfinement crossover of two-magnon bound states scattered by a two-magnon continuum was revealed in the one-dimensional (1D) ferromagnetic chain by the spin entanglement entropy (SEE) analysis. Now, we extend the study to the two-dimensional (2D) and three-dimensional (3D) cases. Although the interactions between magnons in high dimensions are not as effective as in one dimension, two-magnon bound states can still survive around the corners of the Brillouin zone (BZ). In 2D or 3D square lattices, the bound states reduce their dimensionality to be 1D bound states at the BZ edges, which are bound only along the direction parallel to the BZ edge. This is verified by examining the relation between the magnon separation d and the intercept D of the SEE, which is found to satisfy the 1D relation $D = \ln d + 1$, but in 2D and 3D lattices. Meanwhile, the 2D bound states satisfy $D = 2 \ln d + 1.3$ in both 2D and 3D lattices. Unlike those in the 1D chain, some bound states will enter the continuum directly rather than cling to its bottom. We find that these immersed bound states are neither preserved nor deconfined completely when just meeting the continuum in finite-size systems, which is similar to what occurs in the 1D chain. Their SEE and magnon separation oscillate with respect to the system size. Therefore, these bound states undergo the oscillating deconfinement crossover in the continuum.

I. INTRODUCTION

Magnon bound states are also called Bethe strings because of their prediction in one-dimensional (1D) quantum magnets by Bethe [1]. In quantum magnets, the propagation of a single spin flip through coupling with neighboring spins is called a magnon excitation. Due to the effective attraction between magnons, multiple magnons can form bound states. An n-string means that n magnons form a bound state, and that state will inevitably collide with other magnons when encountering the continuum of many-magnon excited states. Therefore, the scattering between the bound states and the continuum constitutes a challenging problem involving the many-body interactions.

In Ref. [2], we studied the spin entanglement entropy (SEE) [2–4] of two-magnon bound states in a 1D ferromagnetic Heisenberg chain, which provides reliable reference points due to its exact solvability. The confinement of the bound states is quantified by an increasing SEE with a separation between the two magnons in the bound states as a particle physics analog [2]. Specially, we find an oscillating confinement-deconfinement crossover of the two-magnon bound states when they are immersed in the two-magnon continuum in an alternating ferromagnetic chain [2]. The

oscillation crossover was illustrated by the oscillating scaling behavior of the SEE. The oscillation indicates that the bound states, scattered in the many-particle continuum, will experience a gradual deconfinement crossover rather than a critical phase transition. This is in contrast to the usual belief that the bound state will experience a damping but be preserved from deconfinement when entering the continuum. The string of bound states will be broken eventually but will have to go through a process of oscillation. The concept of confinement was first introduced in particle physics to describe how the constituent particles are bound together to form new particles. In particle physics, the constituent particles in the confined states cannot be isolated and therefore cannot be observed directly in the usual way. Fortunately, the energy scale of confinement in condensed matter physics is not that unreachable. Hence, the special oscillating deconfinement of magnon bound states found here provides a suitable case to understand confinement in quantum spin systems, which reflects the intrinsic many-body features therein.

Although the interactions between magnons in high dimensions are not as effective as in one dimension, the two-magnon bound state has also been acknowledged in high-dimensional lattices in various quantum magnets [5–26]. It is known that, different from one dimension, there are multiple branches of bound states in high-dimensional ferromagnets, and some of the branches will be immersed in rather than below the two-magnon continuum [7,8,17,19]. Hence, interesting

*jxli@nju.edu.cn

issues arise regarding how to tell the difference between the high-dimensional and 1D bound states and characterize the properties of various branches of the two-magnon bound states and whether the oscillating crossover can be extended to high dimensions or deteriorates to be a transition with a critical point instead.

In this paper, we study the two-magnon bound states in two-dimensional (2D) and three-dimensional (3D) square lattices. The bound states exist mainly around the Brillouin zone (BZ) corner and approach the two-magnon continuum when dispersing from the corner to the center of the BZ. Since the two magnons can be bound along the bonds of different orientations, there are two branches and three branches of bound states in 2D and 3D square lattices, respectively [8]. Moreover, by studying the orientation of bound states, they can be distinguished along different momentum paths. Particularly, some bound states are bounded in only a certain direction rather than in all directions, as if they were lower-dimensional bound states while in the higher-dimensional space [27]. In particular, there is reduced dimensionality of bound states along the BZ edges and surfaces. For example, in the 2D lattice the 1D-like bound states along the BZ edge from (π, π) to $(\pi, 0)$ appear to be bound in the y direction. In the 3D lattice, along the BZ edge from (π, π, π) to $(\pi, \pi, 0)$, the highest-energy branch of bound states behaves as 1D bound states. Also, in the 3D lattice, at the BZ surface along (π, π, π) to $(\pi, 0, 0)$, the branch with the highest energy behaves like 2D bound states.

To further understand the properties of these bound states, we perform a SEE analysis [2]. We showed previously that the scaling of the SEE for two-magnon excitations will have a nonzero intercept D due to the interactions between magnons, and it constitutes a correction to the natural logarithm law of the SEE [2]. In particular, it was found that the intercept is related to the average separation d between two magnons in the bound state. For the normal bound states along the path from (π, π) to $(0,0)$ in the 2D lattice, the two branches of bound states are explicit 2D bound states, as their separations are equal along the x and y directions. We show that their intercept of the SEE versus the separation has an asymptotic behavior to $D = 2 \ln d + 1.3$, where the prefactor 2 denotes their 2D character. On the other hand, the reduced dimensionality of bound states is also revealed by the SEE analysis. The intercept-separation relation of the higher-energy branch along (π, π) to $(\pi, 0)$ is exact, $D = d \ln d - (d - 1) \ln(d - 1)$, which is the same as that in the 1D chain [2] and will be $\ln d + 1$ in the continuum limit.

A similar SEE analysis is also applied to the 3D lattice. The 1D bound state exists on the edge along the (π, π, π) to $(\pi, \pi, 0)$ direction, and its intercept-separation relation is in good agreement with $D = d \ln d - (d - 1) \ln(d - 1)$. At the BZ surface from (π, π, π) to $(\pi, 0, 0)$, the bound states have nonzero separations in the y and z directions. Their intercept-separation relation approaches $2 \ln d + 1.3$, which is the relation for the 2D bound states. Therefore, these bound states at the BZ surface are 2D bound states. The bound states along (π, π, π) to $(0,0,0)$ are definite 3D bound states, and their intercept-separation relation is about $D = 2.7 \ln d + 1.4$.

From the energy spectra of two-magnon excitations, the bound states will either cling to the bottom of the two-magnon
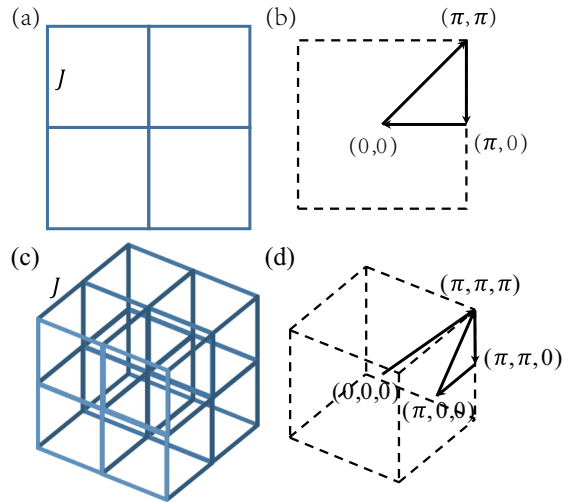
FIG. 1. Illustration of the ferromagnetic Heisenberg model in (a) 2D and (c) 3D square lattices. BZ and high-symmetry points and lines of (b) 2D and (d) 3D square lattices.

continuum or enter the continuum directly after dispersing from the BZ corner [8]. Thus, some bound states will be inevitably immersed in the continuum. This is different from the situation in the 1D ferromagnetic spin chain, where the bound states cling to only the bottom of the continuum. From the spectral perspective, the immersed bound state will spread its spectral weight in the continuum and appears as a heavily suppressed and broad peak. So it is hard to explore the nature of decayed or deconfined immersed bound states from the spectra. We show that the SEE scaling for the immersed bound states exhibits an oscillation with the system size in both finite 2D and 3D lattices. Meanwhile, the separation of the two magnons in the immersed bound states shows a similar oscillation. The clear oscillation of both the SEE and the separation implies that the bound states have to experience an oscillating deconfinement crossover in both 2D and 3D systems that is similar to the oscillating crossover for the deconfinement of the bound states in the 1D alternative ferromagnetic chain [2].

II. MODEL AND METHOD

The Hamiltonian of the spin-1/2 ferromagnetic Heisenberg model on a square lattice is

$$H = -J \sum_{\langle ij \rangle} \mathbf{S}_i \cdot \mathbf{S}_j, \tag{1}$$

where only the nearest bonds $\langle ij \rangle$ are included. The ferromagnetic ground state is chosen to be $|F\rangle = |\uparrow \cdots \uparrow\rangle$. The 2D and 3D square lattices and the corresponding BZ are illustrated in Fig. 1.

Excitations in the space with one spin flip $|r\rangle = S_r^- |F\rangle$, known as magnons, are solved as $|o_k\rangle = \frac{1}{\sqrt{N}} \sum_r e^{ik \cdot r} |r\rangle$, where k is the wave vector of the magnon. Thus, excitations in the space with two spin flips $|r_1, r_2\rangle = S_{r_1}^- S_{r_2}^- |F\rangle$ can be regarded as two-magnon excitations. If there is no interaction between magnons, two magnons with wave vectors k_1 and k_2 will simply form a two-particle continuum satisfying $E_k = E_{k_1} + E_{k_2}$ and $k = k_1 + k_2$. In fact, since the interactions

between magnons will result in the deviation of the momenta from the values of the one-magnon wave vectors k_1 and k_2, two-magnon excitations are not as simple as a two-particle continuum. Fortunately, total momentum k is still a good quantum number due to the translational symmetry, so we can diagonalize H in the subspace with a certain momentum k, and the eigenstates read

$$|t_k\rangle = \sum_{r_1, r_2} \psi_k(r_1, r_2)|r_1, r_2\rangle, \qquad (2)$$

where $\psi_k(r_1, r_2)$ is the coefficient obtained from the exact diagonalization (Appendix A). There are two kinds of solutions in the space for the two spin flips. One is the two-magnon continuum, where the two-magnon excitations deviate from the two free magnons only a little and can be considered two individual particles. The other is the bound state. The two-magnon bound state can be regarded as the confinement of two magnons which not only are spatially close to each other but also bear rich entanglement [2].

A. Magnon pair correlation spectra

The bound states are hard to identify with conventional spin-spin correlation functions due to their negligible spectral weight. As is known, the two magnons in a bound state are always paired along a bond. To observe the bound states, we can check the magnon pair correlation functions, whose spectra are given by

$$P^\alpha(\omega, k) = -\frac{1}{N\pi} \sum_r \text{Im}\left[\sum_{t_k} \frac{|\langle F|S_r^+ S_{r+\delta\alpha}^+|t_k\rangle|^2}{\omega - E_k + i0^+} \right] e^{ik\cdot r}, \quad (3)$$

where $|t_k\rangle$ and the corresponding E_k are solved by the exact diagonalization and α indicates the direction of the bond $\langle r\, r + \delta\alpha \rangle$ along which the two magnons are paired. For high-dimensional square lattices, since two magnons can pair along different bonds, the bound states manifest themselves as different branches. Therefore, we calculate $P^x(\omega, k)$ and $P^y(\omega, k)$ for the 2D model and $P^x(\omega, k)$, $P^y(\omega, k)$, and $P^z(\omega, k)$ for the 3D model.

B. Spin entanglement entropy

Quantum entanglement is used to understand many-body systems [28–34]. One of the best ways to quantify the entanglement is to calculate the entanglement entropy. Therefore, we calculate the SEE to characterize spin excitations and the confinement of the bound states [2–4]. Unlike the traditional entanglement defined in real space, the SEE is based on a bipartition of the system into different spin regions. For instance, the 1D spin chain can be viewed as a two-leg ladder, with the upper leg representing spin up and the lower leg representing spin down. The SEE is then defined by partitioning the system into these two legs. Therefore, the SEE of two-magnon excitations can be obtained with the Schmidt decomposition of their wave functions (2) with respect to this bipartition,

$$S = \sum_{r_1, r_2} -\psi(r_1, r_2)^2 \ln[\psi(r_1, r_2)^2], \qquad (4)$$

and its difference from the ground state can be used to analyze the excitations. As one of their intrinsic attributes, the scalings

of SEEs can distinguish different excitations. Since the spin-up and -down space of magnons has to be entangled at every site to serve the spin-flipping excitations, the SEE of magnons will be logarithmically divergent from the system size N in the thermodynamic limit. The standard $\ln N$ behavior aptly illustrates the single-entity property of one magnon. If there are two free magnons, the SEE is expected to be $2 \ln N$, which is a simple sum of that of each magnon. But when the two magnons are bound together, the SEE of the new quasiparticle of the bound state is [2]

$$S = \ln N + D. \qquad (5)$$

As a result of the inevitable interactions between magnons, a nonzero intercept D exists and acts as the correction to the natural logarithm law of the SEE. In particular, it can be taken to reflect the confinement of two magnons in the bound states [2].

C. Two-magnon separation

One of the major features of bound states is the spatial proximity of magnons in the bound states, so we also discuss the separations of the two magnons in the bound states as a supplement to the SEE analysis. The separation is defined as the average distance between two magnons with the periodic boundary condition in different dimensions,

$$d^\alpha = \sum_{r_1, r_2} \min(|r_2^\alpha - r_1^\alpha|, L^\alpha - |r_2^\alpha - r_1^\alpha|)\psi(r_1, r_2)^2, \quad (6)$$

where L^α is the length of the lattice in the α direction. The separation in 2D and 3D square lattices is the simple sum of d^α,

$$d = \sum_\alpha d^\alpha. \qquad (7)$$

This separation can be interpreted as the minimum number of bonds to connect the two magnons. For bound states, the separation is convergent, while for two free magnons, the separation increases with the system size. When the bound state is merging into the continuum, its oscillating deconfinement crossover is also embodied in the oscillation of the separation [2].

We have shown that the intercept of the SEE of a 1D bound state has a relation to the two-magnon separation [2],

$$D = d \ln d - (d - 1)\ln(d - 1). \qquad (8)$$

The increasing of the SEE with the separation d implies that the larger the separation is, the more entangled the two magnons are. As a particle physics analog, it could be attributed to the confinement of the bound states. In the continuum limit, Eq. (8) will approach $\ln d + 1$.

III. TWO-DIMENSIONAL SQUARE LATTICES

We begin with the 2D square lattice. The energy spectra of two-magnon excitations are shown in Fig. 2(a). Below the two-magnon continuum denoted by gray shaded regions, there are two branches of two-magnon bound states, denoted by different colored lines. To distinguish the bound states, we calculate the pair correlation spectra of magnons along different bonds, and the results are presented in Fig. 2(b) for
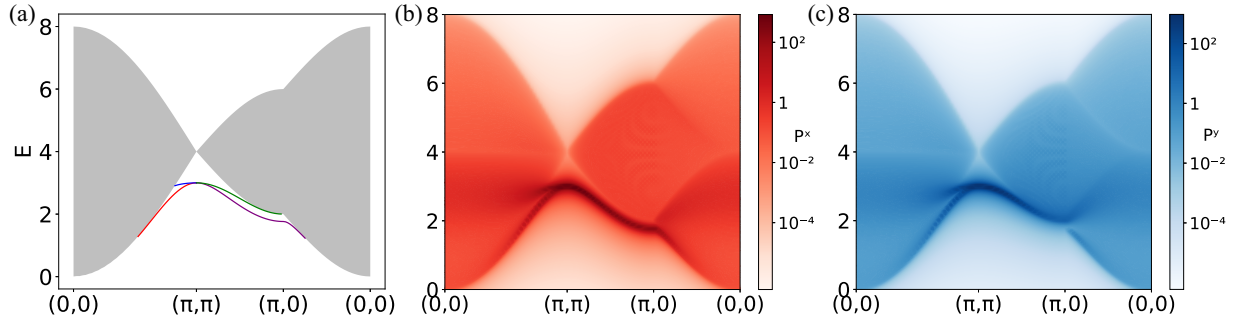
FIG. 2. (a) Energy spectra of two-magnon excitations in the 2D square lattice with system size $L \times L = 80 \times 80$. The two-magnon continuum is denoted by the gray shading, and the two-magnon bound states are denoted by the colored lines. Magnon pair correlation spectra (b) $P^x(\omega, k)$ and (c) $P^y(\omega, k)$ for the two-magnon excitations in a 2D square lattice.

P^x and Fig. 2(c) for P^y. The bound states with highest spectral intensities locate in the BZ corner (π, π), where the two branches are degenerate [8]. Then, the bound states disperse down to the BZ center with gradually decreasing spectral intensities. From (π, π) to $(0,0)$, both branches of bound states have the same spectral weights in both the P^x and P^y spectra. The higher-energy branch enters directly into the continuum at about $(4\pi/5, 4\pi/5)$, which is in agree with the threshold point $(2 \arccos(4/\pi - 1), 2 \arccos(4/\pi - 1))$ at which the branch merges with the continuum in the thermodynamic limit [8], and then spreads its spectral weight rapidly by transferring it into the continuum. This suggests that the bound states are damped or deconfined when immersed in the continuum. The lower branch appears to extend to zero energy and clings to the lower boundary of the continuum [8]. However, the bound states are found to be dissolved at about $(\pi/2, \pi/2)$ in the calculations with system size $L \times L = 80 \times 80$, which is caused by the finite-size effect. Along another path from (π, π) to $(\pi, 0)$, the two branches behave quite differently at the BZ edge. The higher-energy branch of bound states has higher intensities in the P^y spectra, while the lower-energy branch has higher intensities in the P^x spectra. Furthermore, the higher-energy branch clings to the bottom of the continuum until $(\pi, 0)$ and then becomes immersed in it. After the $(\pi, 0)$ point and along the path from $(\pi, 0)$ to $(0,0)$, the lower branch contributes intensities in both the P^x and P^y spectra and is always situated below the continuum.

To quantitatively identify these bound states, we calculate their SEE according to Eq. (4). For a system of size $L \times L$, the SEEs of both the bound states and continuum are verified to satisfy the logarithmic relation with respect to system size:

$$S_{\text{bound}} = 2 \ln L + D \qquad (9)$$

for the bound states and

$$S_{\text{continuum}} = 4 \ln L + D \qquad (10)$$

for the continuum. The intercept D, as a correction to the $\ln L$ scaling, is due to the many-body interactions between magnons. The intercepts of the continuum in Eq. (10) are mostly around -1 because of the indistinguishability and coherence of the magnons [2]. On the other hand, the intercepts of the bound states in Eq. (9) can be used to characterize the confinement of the bound states by examining their relation to the two-magnon separation [2]. The calculated results for this

relation are illustrated in Fig. 3(a), where the colored lines denote the results for the bound states labeled by the same color in Fig. 2(a). The bound states denoted by both the red and purple lines approach the asymptote scaling relation $2 \ln d + 1.3$ with the increase of the separation d; $2 \ln d + 1.3$ can be explained as $\ln S + \text{const}$, where $S \propto d^2$ is the area enclosing the two magnons. Therefore, the 2D bound states are different from 1D bound states, which can be simply pictured as being bound by a string, and the more rapid divergence of the SEE implies more unstable bound states in two dimensions. In short, the term $2 \ln d$ indicates that these bound states have a 2D character. From Fig. 2, one can see that the bound state denoted by the blue line extends to only a limited momentum space near (π, π) along the diagonal direction before it enters the continuum. Therefore, we can calculate the separation d for only a limited range to approach the asymptotic behavior. Nevertheless, from its tendency shown in Fig. 3(a) and the close-up in the inset, it is expected to approach $2 \ln d + 1.3$. Thus, we have shown that, among the four branches of
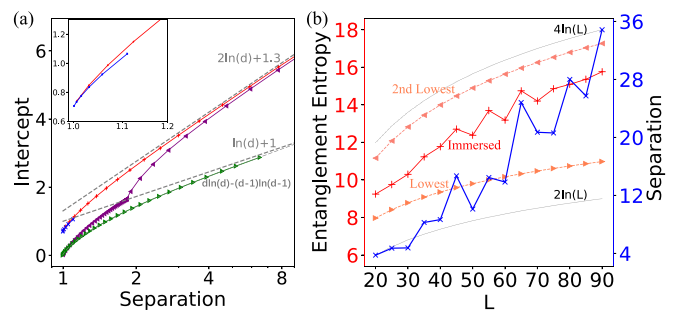
FIG. 3. (a) Intercept-separation relations of the bound states in the 2D square lattice. The colors are in line with those in Fig. 2(a). The inset is a zoom-in image in the range of $d = (1.0, 1.2)$. The intercept of the SEE and the two-magnon separation in the bound states are independent of system size, so they are calculated in an $L \times L = 80 \times 80$ lattice. (b) Scaling of the SEE of the immersed bound state at $(4\pi/5, 4\pi/5)$. For the determination of the immersed bound state, see the text. The red line indicates the oscillating SEE, and the blue line indicates the oscillating two-magnon separations of the immersed bound state. The lowest state is the branch of the bound state with the lowest energy, which is preserved below the continuum, and the second-lowest state is the state at the bottom of the continuum. The gray lines are the reference lines.

two-magnon bound states, the three branches denoted by the red, purple, and blue lines exhibit 2D character. For the fourth branch, we suggest that this bound state (denoted by the green line) will behave as a 1D bound state based on the magnon pair correlation spectra presented in Fig. 2(a). This spectral analysis is verified by the SEE calculation. Figure 3(a) shows that the intercept of the SEE follows exactly the relation $D = d \ln d - (d - 1) \ln(d - 1)$, which is in agreement with that in the 1D ferromagnetic chain. Moreover, the presence of nonzero separations only in the y direction also indicates that the states are bound only in the y direction. Therefore, we conclude that only the bound states along the BZ edge, i.e., from (π, π) to $(\pi, 0)$ [see Fig. 1(b)], are 1D bound states, although they are in 2D lattices.

We also note that the intercept of the bound states denoted by the purple line seems to tend to $\ln d + 1$, which is the continuum limit of $D = d \ln d - (d - 1) \ln(d - 1)$, when along the BZ edge from (π, π) to $(\pi, 0)$, as shown for $d < 2$ in Fig. 3(a). We find that their separation are nonzero in both directions, and especially, those in the x direction are exact, $d^x = 1$, so they have the highest intensities in P^x and look like 1D bound states. However, the real 1D bound state denoted by the green line has separation in only one direction with $d^x = 0$; that is, the two magnons are bound in one dimensions. Furthermore, as the separation in the y direction increases gradually, it deviates from the exact relation $D = d \ln d - (d - 1) \ln(d - 1)$. Then, when turning to the BZ center after $(\pi, 0)$, it approaches $2 \ln d + 1.3$ rapidly. Consequently, we think that the bound states labeled with the purple line are still 2D bound states but are just bound very tightly in the x direction.

After identifying the bound states, we turn to study the fate of the bound states immersed in the continuum. As shown in Fig. 2(a), the bound states denoted by the blue line enter the continuum rather than clinging to the continuum like others. In this case, damping or deconfinement of the bound state is expected when it enters the continuum at about $(4\pi/5, 4\pi/5)$. Since the immersed bound state hybridizes with the continuum, it is difficult to identify this state using the usual analysis based on the spectral function shown in Fig. 2(a). However, in the SEE analysis, the prefactor of the natural logarithm law scaling for the bound states is only half of the SEE of continuum states, as shown by Eqs. (9) and (10). When the bound states merge into the continuum, although the exact ratio no longer holds, the immersed states will still have the minimum SEE. So the state with the smallest SEE is identified as the bound state immersed in the continuum. In Fig. 3(b), we present our results for the scalings of three typical SEEs of the two-magnon excitations at $(4\pi/5, 4\pi/5)$, where the state immersed in the continuum is determined above, the lowest state is the bound state below the continuum with a gap [denoted by the red line in Fig. 2(a)], and the second-lowest state is at the bottom of the continuum. One can see that the SEE of the lowest state has a standard $2 \ln L + D$ scaling like that for the bound states, and the second-lowest state has a $4 \ln L + D$ scaling like that for the two-magnon continuum. In contrast, the SEE of the immersed state [shown by the red line in Fig. 3(b)] does not agree with either $2 \ln L + D$ or $4 \ln L + D$ and oscillates with the system size. Its behavior is similar to that in the 1D ferromagnetic chain [2]. This oscillation
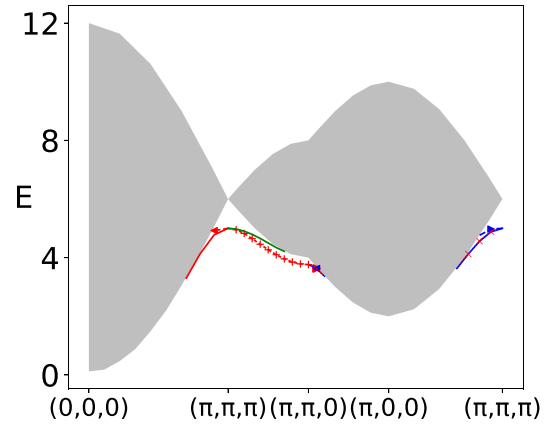
FIG. 4. Energy spectra of two-magnon excitations in the 3D square lattice with system size $L \times L \times L = 20 \times 20 \times 20$. The two-magnon continuum is denoted by the gray shading, and two-magnon bound states are denoted by the colored lines.

indicates that the bound state cannot be considered conventionally to be preserved as a quasiparticle with damping or deconfined into two individual magnons after encountering the continuum. Obviously, the two magnons confined as a bound state will experience an oscillating crossover before being deconfined. Accordingly, the separation of two magnons in the immersed bound state also exhibits an oscillation, as shown by the blue line in Fig. 3(b). The oscillation of the two-magnon separation also characterizes the deconfinement crossover [2]. Moreover, the fact that the separation does not approach $d = L/2$, which is the average distance between two free magnons, indicates that the immersed state is not yet deconfined completely. It is also noted that the SEE oscillation seems to fade away when $L > 80$. Given that the oscillation of the two-magnon separation is still severe when $L > 80$, it is reasonable that the oscillation of the SEEs merely meets the node at about $L = 85$. Therefore, we show that the bound state will undergo an oscillating crossover from a confined state to a deconfined state when it enters the two-magnon continuum.

IV. THREE-DIMENSIONAL SQUARE LATTICES

The 3D square lattice and the corresponding BZ are shown in Figs. 1(c) and 1(d), respectively. In Fig. 4, we show the energy spectra of two-magnon excitations in the 3D square lattice. As the magnon-magnon interactions in the high-dimensional system are not as prominent as in the 1D system, the bound states in fact assemble around the BZ corner in 3D square lattices [7,8,17]. There are three branches of bound states since the magnons can form pairs along three different bonds, and the three branches are degenerate at the BZ corner (π, π, π) [8]. Along the path from (π, π, π) to $(0,0,0)$, the branch with the lowest energy clings to the continuum until it cannot be identified from the spectra, and the other two degenerate branches disperse from (π, π, π) and then enter the continuum directly. Along the edge from (π, π, π) to $(\pi, \pi, 0)$, the lowest two branches are degenerate, and the other branch, shown by the green line in Fig. 4, clings to the continuum and then enters it at $(\pi, \pi, 0)$. When turning
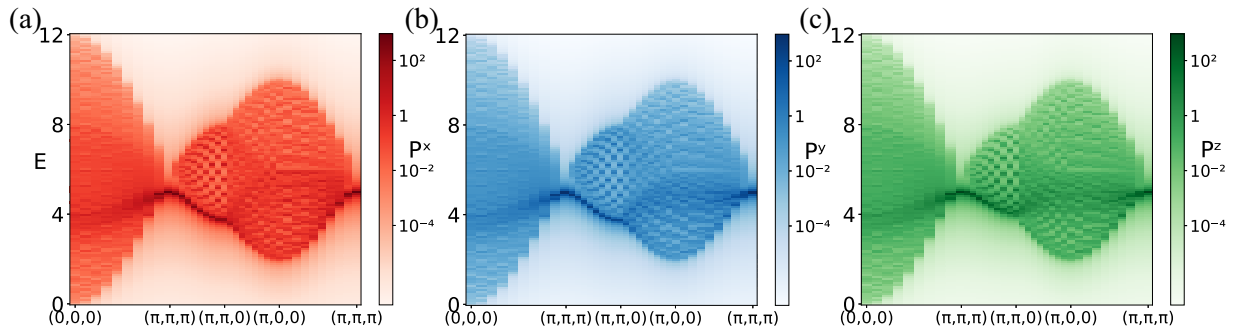
FIG. 5. Magnon pair correlation spectra in the 3D square lattice with system size $L \times L \times L = 18 \times 18 \times 18$: (a) $P^x(\omega, k)$, (b) $P^y(\omega, k)$, and (c) $P^z(\omega, k)$.

to $(\pi, 0, 0)$ from $(\pi, \pi, 0)$, the degeneracy of the lowest two branches is lifted. At the surface from (π, π, π) to $(\pi, 0, 0)$, all three branches are nondegenerate, although the two lower branches are very close. Among these three branches, after dispersing from (π, π, π) the highest branch enters the continuum soon and then cannot be identified.

Now that we have discussed the dispersions of the bound states, let us examine the properties of the three branches of bound states based on the magnon pair correlation spectra. The results are presented in Figs. 5(a)–5(c) for P^x, P^y, and P^z, respectively. Similar to those in the 2D case, the bound states with the highest spectral intensities locate at the BZ corner (π, π, π). Along the diagonal path from (π, π, π) to $(0,0,0)$, one can identify a branch with high intensities; then it enters the continuum and dissipates with only a hint of the original state. From the dispersion relation shown in Fig. 4, we can ascribe this branch to the two degenerate bound states with higher energy discussed above. These bound states distribute their spectral weights equally in the P^x, P^y, and P^z spectra. Along this diagonal path, the third branch as a whole is not very easy to distinguish from the continuum due to the limited lattice sizes we can treat, but we can still find it near (π, π, π), and it also displays an equal spectral weight distribution among P^x, P^y, and P^z. Therefore, these bound states along the diagonal direction of the BZ have the usual 3D character. At the BZ surface from (π, π, π) to $(\pi, 0, 0)$, the branch with the highest energies has intensities in only the P^y and P^z spectra, as shown in Figs. 5(b) and 5(c). So they seem to be 2D bound states. Along the BZ edge from (π, π, π) to $(\pi, \pi, 0)$, the two lower-energy degenerate branches are distributed in the P^x and P^y spectra, while, the highest-energy branch exhibits intensities only in the P^z spectra. Hence, at the BZ edge, the two lower-energy branches seem to be 2D bound states, while the highest-energy branch consists of 1D bound states.

As shown in the last section, different bound states have different intercept-separation relations. So we examine the relation like we did for the 2D system, and the results are shown in Fig. 6(a). The lines and the markers denote the bound states, with the colors and symbols corresponding to those shown in Fig. 4. The separations of the bound states along the (π, π, π) to $(\pi, \pi, 0)$ direction denoted by the green line are nonzero only in the z direction, and their intercept-separation relation is in good agreement with $D = d \ln d - (d-1) \ln(d-1)$. So the SEE scaling analysis evidences that these bound states

at the BZ edge are 1D bound states. The bound states at the BZ surface from (π, π, π) to $(\pi, 0, 0)$ denoted by the blue line have nonzero separations in the y and z directions. Their intercept-separation relation, as shown by the blue line in Fig. 6(a), approaches $2 \ln d + 1.3$, which is the relation for 2D bound states. Therefore, these bound states at the BZ surface are 2D bound states. The bound states from (π, π, π) to $(0,0,0)$ denoted by the red line are definitely 3D bound states with separations $d^x = d^y = d^z$. Because of the limited computing power, there are only two states to simulate the relation, which is about $2.7 \ln d + 1.4$. Although this relation approximates the intercept-separation relation for 3D bound states, it is, in fact, hard to determine the exact relation due to the limitation of the computing capacity. The bound states at the BZ edge from (π, π, π) to $(\pi, \pi, 0)$ denoted by the red line have the exact relation $d^x + d^y = 1$ for the separation of two magnons in the x and y directions and a d^z increasing from zero. So they have a tendency toward $\ln d + 1$ but deviate from it when turning to $(\pi, 0, 0)$, as shown by the red pluses in Fig. 6(a). In addition to the 2D bound states with higher energies at the BZ surface from (π, π, π) to $(\pi, 0, 0)$ denoted by the blue line, the lower-energy bound states denoted by the red line have exact separation in the x direction, $d^x = 1$. So their relations appear to be 2D bound states with a tendency
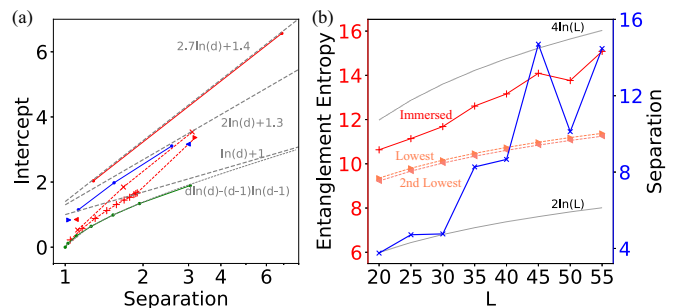
FIG. 6. (a) Intercept-separation relations of the bound states in the 3D square lattice. The lines and the markers are in line with the corresponding bound states in Fig. 4. (b) Scaling of the SEE of the immersed bound state at $(\pi, 4\pi/5, 4\pi/5)$. The red line indicates the oscillating SEE, and the blue line indicates the oscillating separations of the immersed bound state. The lowest and second-lowest states are the other two branches of the bound states with the lowest and second-lowest energies, which are preserved below the continuum.

toward $2 \ln d + 1.3$. Despite this, the bound states denoted by the red line should be 3D bound states that are merely bound too tightly in some directions. In addition, some individual bound states, which are hard to simulate using the relation, are shown as red and blue triangles in Fig. 6(a). In summary, based on the combined analysis of the magnon pair correlation spectra and the spin entanglement entropy, we elaborate that the bound states denoted by the green line in Fig. 4 appear to be 1D bound states, those denoted by the blue lines appear to be 2D bound states, and those denoted by the red lines appear to be 3D bound states. In summary, there are 1D bound states at the BZ edge and 2D bound states at the BZ surface in the 3D lattice.

From the magnon pair correlation spectra shown in Fig. 4, one can see that there are branches of bound states which will eventually enter the continuum. They have higher energies along the corresponding paths, denoted by the red marked line along the (π, π, π) to $(0,0,0)$ direction, the green line along the (π, π, π) to $(\pi, \pi, 0)$ direction, and the blue dashed line along the (π, π, π) to $(\pi, 0, 0)$ direction. Due to the addition of one more dimension, the identification of the position where the bound states are immersed becomes much less possible except at some special k points. Therefore, to check the deconfinement transition of the immersed bound states, we will choose the immersed bound state at $(\pi, 4\pi/5, 4\pi/5)$ as an example. At $(\pi, 4\pi/5, 4\pi/5)$, the higher-energy branch of bound states begins to encounter the continuum and exhibits diffusive intensities. We calculate the SEE and the separation of two magnons with a $4 \times L \times L$ system, and the results are shown in Fig. 6(b). The red line denotes the result for the immersed bound state, while the dashed orange lines label the two branches with the lowest and second-lowest energies at the same k, and the blue line denotes the separation of the two magnons in the immersed state. The SEEs of the bound states with the lowest and second-lowest energies are the standard $2 \ln L + D$ of bound states. The SEE of the immersed bound state shows the characteristic oscillation with L. Correspondingly, the two-magnon separation also shows an oscillation. Therefore, the deconfinement of the bound states in 3D systems also has to experience the oscillating crossover.

V. DISCUSSION AND CONCLUSION

Two-magnon bound states involve the motion of two magnons but act as a single emergent entity. The spin entanglement entropy analysis illustrates that the two magnons are confined in the bound state by unveiling the fact that the intercept of the SEE increases monotonically with the separation between magnons [2]. It is known that bound states are expected to decay when encountering the inevitable continuum of magnons. From the spectral perspective, this decay is signaled by the suppressed quasiparticle peak and the increased full width at half maximum. However, with the help of the SEE, we were able to analyze the process of the deconfinement quantitatively. The SEE study revealed an unusual oscillating crossover rather than a transition with a critical point for the bound states immersed in the two-magnon continuum. The oscillation indicates that the deconfinement of the bound states is such a complicated process that it deserves further investigation. Moreover, the oscillating deconfinement

crossover is probably not a feature exclusive to magnon bound states. In the ferromagnetic Luttinger liquid of edge states in graphene, magnons have been shown to deconfine into spinons in the Stoner continuum [3]. As we show in Appendix B, the SEE and the two-spinon separation of the immersed mode at $\pi/24$, which is near the Goldstone mode, also exhibit a similar oscillation with a system size up to lattice size $N \sim 4800$. So the deconfinement of a magnon into two spinons in the ferromagnetic edge states of graphene also experiences an oscillating process when the spin-flip excitations deviate from the Goldstone mode. Another possibility is related to the phenomenon of the anomalous spectra of high-energy magnon excitations at certain k points observed in quantum antiferromagnetic magnets [35–47]. A possible explanation for the anomalies is partial deconfinement of magnons when they are coupled to the two-spinon continuum [36,48–60]. We expect that this kind of deconfinement of magnons into spinons will experience a similar oscillating crossover. Since all the current calculations are carried out on systems with a finite size, it is hard to exclude the possibility that the oscillating deconfinement crossover results from the finite-size effect. However, in most cases, the oscillations are not weakened and are even enhanced with the increase of the system size. Especially in the 1D chain [2], the oscillations are distinctly enhanced even when the chain length $N > 2000$. This behavior can hardly be ascribed to a simple finite-size effect which should vanish asymptotically as the system size increases. Thus, even if the oscillation is forbidden in the thermodynamic limit, it should be observed in a nanosize system with thousands of sites. Recently, ultracold atoms offered an ideal setting in which to find magnon bound states by tracking the spin dynamics with single-spin and single-site resolution [61,62]. It was implied that the deconfinement oscillations could be detected in such experiments and adapted to possible applications. Admittedly, as an unusual phenomenon, the oscillating crossover of the deconfinement of magnon bound states remains to be verified in the thermodynamic limit in the future.

In conclusion, we studied the properties and deconfinement crossover of the two-magnon bound states in 2D and 3D square lattices based on a combined analysis of the magnon pair correlation spectra and the spin entanglement entropy. There are two and three branches of bound states in 2D and 3D lattices, respectively. The SEE of bound states in one dimension is related to the separations between magnons as $D = \ln d + 1$. The two magnons appear to be bound by a string along the one dimension. In two dimensions, the SEE of bound states turns out to be related to the area enclosing the two magnons, so the relation involves a square of separations as $D = \ln d^2 + \text{const}$, where d^2 stems from the area enclosing the magnons. It seems that 2D bound states are not as simple as those in one dimension, which can be pictured as being bound by a string. In this case, we may guess that the 3D bound states are related to the volume of two magnons. Unfortunately, we did not achieve $D = \ln d^3 + \text{const}$ for 3D bound states to prove this speculation. However, the coefficient of 2.7 in the relation $D = 2.7 \ln d + 1.4$ suggests that the bound states in three dimensions are complicated, and the enlargement implies that the bound states become more fragile in high dimensions. On the other hand, with the SEE

analysis, we verified that even in the high-dimensional lattices some magnons tend to be bound only in certain directions, such as the BZ edges and surfaces. Although the attraction between magnons in high dimensions is not as efficient as that in one dimension, there are still special 1D bound states at the BZ edges and 2D bound states at the BZ surface around the BZ corner that are preserved from being deconfined into individual magnons. The intercept of the SEE for the 1D bound states at the BZ edges satisfies the exact relation with the separation d of two magnons $D = d \ln d - (d-1) \ln(d-1)$, which is the same as that found in the case of a 1D chain [2], and that for the 2D bound states at the BZ surface satisfies $D = 2 \ln d + $ const. These bound states exist in certain momentum regions and will dissolve in the continuum. Different from the 1D case, the higher-energy branches of magnons will enter the continuum rather than cling to the continuum. We showed that the intercept of their SEE and the magnon separation exhibits an oscillation with the system size when entering the continuum. So these immersed bound states are neither preserved nor deconfined completely when entering the continuum and experience the oscillating deconfinement crossover. The oscillation behaviors were also shown in the ferromagnetic edge states of graphene and in the 1D alternative ferromagnetic chain [2]. Therefore, we suggest that the oscillating deconfinement of collective modes immersed in a many-particle continuum could be a general property.

APPENDIX A: EXACT DIAGONALIZATION WITH THE MOMENTUM BASIS

Since the translation symmetry is present, the system can be divided according to the eigenstates of the translation operator T,

$$T|a_k\rangle = e^{ik}|a_k\rangle, \tag{A1}$$

where $|a_k\rangle$ can be constructed using a reference state and all its translations,

$$|a_k\rangle = \frac{1}{\sqrt{N_a}} \sum_{r=1}^{L} e^{ikr} T^r |a\rangle,$$

where $T^L = 1$ is the periodic boundary condition and N_a is the normalization constant. Since the periodicity of the state $|a\rangle$ may be less than L,

$$T^{L_a}|a\rangle = |a\rangle. \tag{}$$

Then the normalization constant $N_a = N^2/L_a$.

It is then clear that the momentum states are orthogonal, and we can construct the Hamiltonian matrix in the basis

with momentum states referring to momentum k. The matrix elements of the Hamiltonian read

$$\langle b_k|H|a_k\rangle = \langle b|H|a\rangle e^{-ikl} \sqrt{\frac{N_b}{N_a}}, \tag{A2}$$

where l satisfies $H|a\rangle \propto T^{-l}|b\rangle$.

To calculate the excitations in the space with two spin flips, the reference state is chosen to be $|a\rangle = |r_1, r_2\rangle = S_{r_1}^- S_{r_2}^- |F\rangle$, with $|F\rangle$ being the ferromagnetic ground state as defined in the main text. Then the eigenstate of the excitations reads

$$|t_k\rangle = \frac{1}{\sqrt{N_a}} \sum_{r_1, r_2, r} \phi_k(r_1, r_2) e^{ikr} T^r |r_1, r_2\rangle, \tag{A3}$$

where $\phi_k(r_1, r_2)$ is the eigenvector of the matrix of the Hamiltonian (A2).

APPENDIX B: OSCILLATING DECONFINEMENT CROSSOVER OF THE MAGNONS IN FERROMAGNETIC EDGE STATES OF GRAPHENE

In Ref. [3], we studied the spin excitations of the ferromagnetic edge states of graphene. Different from traditional magnets, the well-defined magnons are absent, and the spin excitation spectra exhibit an entire continuum. An SEE analysis showed that the magnons were deconfined into spinons in the Stoner continuum except for the zero-energy Goldstone mode. The immersed magnons can be identified by the broad peaks in the SEE spectra in Fig. 3 of Ref. [3]. When carefully examining these modes, one will find an unusual oscillation in the SEE as a function of momentum near the Goldstone mode in Fig. 3(c) of Ref. [3]. To check this observation, we study the SEE of the mode at momentum $\pi/24$, and the numerical results are shown in Fig. 7. The oscillations of the SEE and the two-spinon separation show that the deconfinement of the magnons also has to experience an oscillating crossover.
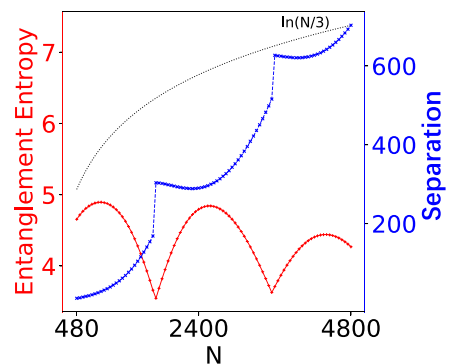
FIG. 7. Scaling of the SEE of the immersed mode at $\pi/24$ in the ferromagnetic edge states of graphene. The red line indicates the oscillating SEE, and the blue line indicates the oscillating separation between the particle and hole in the mode. The gray line denotes the divergent SEE for magnons.

[1] H. Bethe, Z. Phys. **71**, 205 (1931).

[2] Z.-Y. Dong and J.-X. Li, Phys. Rev. B **105**, L220402 (2022).

[3] Z.-Y. Dong, W. Wang, Z.-L. Gu, S.-L. Yu, and J.-X. Li, Phys. Rev. B **102**, 224417 (2020).

[4] Z.-Y. Dong, W. Wang, Z.-L. Gu, and J.-X. Li, Phys. Rev. B **104**, L180406 (2021).

[5] F. J. Dyson, Phys. Rev. **102**, 1217 (1956).

[6] S. Lovesey and E. Balcar, Phys. Lett. A **30**, 84 (1969).

[7] J. Hanus, Phys. Rev. Lett. **11**, 336 (1963).

[8] M. Wortis, Phys. Rev. **132**, 85 (1963).

[9] F. D. M. Haldane, J. Phys. C **15**, L1309 (1982).

[10] B. W. Southern, R. J. Lee, and D. A. Lavis, J. Phys.: Condens. Matter **6**, 10075 (1994).

[11] R. Silberglitt and A. B. Harris, Phys. Rev. Lett. **19**, 30 (1967).

[12] T. Tonegawa, Prog. Theor. Phys. Suppl. **46**, 61 (1970).

[13] M. Takahashi, Prog. Theor. Phys. **46**, 401 (1971).

[14] D. A. Pink and P. Tremblay, Can. J. Phys. **50**, 1728 (1972).

[15] I. Ono, S. Mikado, and T. Oguchi, J. Phys. Soc. Jpn. **30**, 358 (1971).

[16] C. K. Majumdar, J. Math. Phys. **10**, 177 (1969).

[17] A. M. Bonnot and J. Hanus, Phys. Rev. B **7**, 2207 (1973).

[18] T. Oguchi and T. Ishikawa, J. Phys. Soc. Jpn. **34**, 1486 (1973).

[19] R. P. Reklis, Phys. Rev. B **9**, 4939 (1974).

[20] T. Oguchi, J. Phys. Soc. Jpn. **31**, 394 (1971).

[21] H. C. Fogedby, J. Phys. C **13**, L195 (1980).

[22] T. Schneider, Phys. Rev. B **24**, 5327 (1981).

[23] L. Kecke, T. Momoi, and A. Furusaki, Phys. Rev. B **76**, 060407(R) (2007).

[24] X. Qin, F. Mei, Y. Ke, L. Zhang, and C. Lee, Phys. Rev. B **96**, 195134 (2017).

[25] X. Qin, F. Mei, Y. Ke, L. Zhang, and C. Lee, New J. Phys. **20**, 013003 (2018).

[26] F. Letscher and D. Petrosyan, Phys. Rev. A **97**, 043415 (2018).

[27] E. Rastelli, *Statistical Mechanics of Magnetic Excitations* (World Scientific, Singapore, 2013).

[28] L. Amico, R. Fazio, A. Osterloh, and V. Vedral, Rev. Mod. Phys. **80**, 517 (2008).

[29] V. Vedral, Nature (London) **453**, 1004 (2008).

[30] G. Vidal, J. I. Latorre, E. Rico, and A. Kitaev, Phys. Rev. Lett. **90**, 227902 (2003).

[31] X.-G. Wen, Rev. Mod. Phys. **89**, 041004 (2017).

[32] C. Broholm, R. J. Cava, S. A. Kivelson, D. G. Nocera, M. R. Norman, and T. Senthil, Science **367**, eaay0668 (2020).

[33] H.-C. Jiang, Z. Wang, and L. Balents, Nat. Phys. **8**, 902 (2012).

[34] R. Thomale, D. P. Arovas, and B. A. Bernevig, Phys. Rev. Lett. **105**, 116805 (2010).

[35] N. B. Christensen, H. M. Ronnow, D. F. McMorrow, A. Harrison, T. G. Perring, M. Enderle, R. Coldea, L. P. Regnault, and G. Aeppli, Proc. Natl. Acad. Sci. USA **104**, 15264 (2007).

[36] B. Dalla Piazza, M. Mourigal, N. B. Christensen, G. J. Nilsen, P. Tregenna-Piggott, T. G. Perring, M. Enderle, D. F. McMorrow, D. A. Ivanov, and H. M. Rønnow, Nat. Phys. **11**, 62 (2015).

[37] N. S. Headings, S. M. Hayden, R. Coldea, and T. G. Perring, Phys. Rev. Lett. **105**, 247001 (2010).

[38] H. D. Zhou, C. Xu, A. M. Hallas, H. J. Silverstein, C. R. Wiebe, I. Umegaki, J. Q. Yan, T. P. Murphy, J.-H. Park, Y. Qiu, J. R. D. Copley, J. S. Gardner, and Y. Takano, Phys. Rev. Lett. **109**, 267206 (2012).

[39] T. Susuki, N. Kurita, T. Tanaka, H. Nojiri, A. Matsuo, K. Kindo, and H. Tanaka, Phys. Rev. Lett. **110**, 267201 (2013).

[40] J. Ma, Y. Kamiya, T. Hong, H. B. Cao, G. Ehlers, W. Tian, C. D. Batista, Z. L. Dun, H. D. Zhou, and M. Matsuda, Phys. Rev. Lett. **116**, 087201 (2016).

[41] S. Ito, N. Kurita, H. Tanaka, S. Ohira-Kawamura, K. Nakajima, S. Itoh, K. Kuwahara, and K. Kakurai, Nat. Commun. **8**, 235 (2017).

[42] Y. Kamiya, L. Ge, T. Hong, Y. Qiu, D. L. Quintero-Castro, Z. Lu, H. B. Cao, M. Matsuda, E. S. Choi, C. D. Batista, M. Mourigal, H. D. Zhou, and J. Ma, Nat. Commun. **9**, 2666 (2018).

[43] Y. Shirata, H. Tanaka, A. Matsuo, and K. Kindo, Phys. Rev. Lett. **108**, 057205 (2012).

[44] J. Xing, E. Feng, Y. Liu, E. Emmanouilidou, C. Hu, J. Liu, D. Graf, A. P. Ramirez, G. Chen, H. Cao, and N. Ni, Phys. Rev. B **102**, 014427 (2020).

[45] C. Wessler, B. Roessli, K. W. Krämer, B. Delley, O. Waldmann, L. Keller, D. Cheptiakov, H. B. Braun, and M. Kenzelmann, npj Quantum Mater. **5**, 85 (2020).

[46] G. Sala, M. B. Stone, B. K. Rai, A. F. May, D. S. Parker, G. B. Halász, Y. Q. Cheng, G. Ehlers, V. O. Garlea, Q. Zhang, M. D. Lumsden, and A. D. Christianson, Phys. Rev. B **100**, 180406(R) (2019).

[47] G. Sala, M. B. Stone, B. K. Rai, A. F. May, P. Laurell, V. O. Garlea, N. P. Butch, M. D. Lumsden, G. Ehlers, G. Pokharel, A. Podlesnyak, D. Mandrus, D. S. Parker, S. Okamoto, G. B. Halász, and A. D. Christianson, Nat. Commun. **12**, 171 (2021).

[48] F. Ferrari and F. Becca, Phys. Rev. X **9**, 031026 (2019).

[49] C. Zhang and T. Li, Phys. Rev. B **102**, 075108 (2020).

[50] S.-L. Yu, W. Wang, Z.-Y. Dong, Z.-J. Yao, and J.-X. Li, Phys. Rev. B **98**, 134410 (2018).

[51] F. Ferrari and F. Becca, Phys. Rev. B **98**, 100405(R) (2018).

[52] F. Ferrari and F. Becca, J. Phys.: Condens. Matter **32**, 274003 (2020).

[53] T. C. Hsu, Phys. Rev. B **41**, 11379 (1990).

[54] O. F. Syljuåsen and H. M. Rønnow, J. Phys.: Condens. Matter **12**, L405 (2000).

[55] C. M. Ho, V. N. Muthukumar, M. Ogata, and P. W. Anderson, Phys. Rev. Lett. **86**, 1626 (2001).

[56] W. Zheng, J. O. Fjærestad, R. R. P. Singh, R. H. McKenzie, and R. Coldea, Phys. Rev. Lett. **96**, 057201 (2006).

[57] Y. Tang and A. W. Sandvik, Phys. Rev. Lett. **110**, 217213 (2013).

[58] E. A. Ghioldi, M. G. Gonzalez, L. O. Manuel, and A. E. Trumper, Europhys. Lett. **113**, 57001 (2016).

[59] H. Shao, Y. Q. Qin, S. Capponi, S. Chesi, Z. Y. Meng, and A. W. Sandvik, Phys. Rev. X **7**, 041072 (2017).

[60] M. Gohlke, R. Verresen, R. Moessner, and F. Pollmann, Phys. Rev. Lett. **119**, 157203 (2017).

[61] M. Ganahl, E. Rabel, F. H. L. Essler, and H. G. Evertz, Phys. Rev. Lett. **108**, 077206 (2012).

[62] T. Fukuhara, P. Schauß, M. Endres, S. Hild, M. Cheneau, I. Bloch, and C. Gross, Nature (London) **502**, 76 (2013).